Radiative transfer and cloud variability: from remote sensing to climate sensitivity

Howard W. Barker

Meteorological Service of Canada
Cloud Physics Research Division (ARMP), 4905 Dufferin St.
Downsview, ON, Canada M3H 5T4

1. Introduction

For several decades now the large-scale atmospheric modelling community has recognized generally that credible simulation of climate and climatic change requires satisfactory modelling of Earth's radiative and hydrologic budgets (IPCC 1996). This is a tall order given the vast range of horizontal spatial scales that are unresolved in large-scale atmospheric models (LSAMs) and the necessary vertical discretization of the atmosphere. Over the same period, huge stores of global satellite data became available (Ramanathan 1987; Rossow and Schiffer 1999) and have become a keystone for observing climatic change and assessing climate models and their parametrization of subgrid-scale processes. Central to both these main streams of climate research is radiative transfer for cloudy atmospheres. The main point of concern is the near-ubiquitous application in LSAMs and satellite inversion algorithms of 1D radiative transfer models that assume clouds to be plane-parallel and homogeneous (PPH). In actuality, of course, clouds are the antithesis of PPH.

With increasing regularity, theoretical modelling studies demonstrate that radiative transfer models that: i) assume unresolved clouds to be PPH; ii) act on mean values of cloud optical depth τ; and iii) disregard vertical overlap of cloud, are liable to produce substantial, and often systematic, errors in their predicted flux profiles (e.g., Welch and Wielicki 1985; Morcrette and Fouquart 1986; Cahalan et. al 1994; Barker et al. 1999). Clearly then, if cloud properties used by LSAM radiation codes were not *massaged* so as to yield realistic top of atmosphere (TOA) radiation budgets (e.g., Yu et al. 1997), the impact on simulated climate due to use of 1D-PPH codes would be catastrophic. These massaging techniques generally take the form of *ad hoc* adjustments either applied to cloud properties just before entering the radiation routine, or they are integrated, more insidiously, into other parametrized processes. Regardless of how they are realized, momentum is building to eradicate such *tunings* and abandon the PPH paradigm in favour of radiative transfer codes and cloud schemes that address directly unresolved cloud structure. It is hoped that then LSAMs will represent cloud-radiation feedbacks better and thereby reduce the uncertainty that currently dogs climate prediction.

Similar criticisms are leveled at passive remote sensing techniques that use data from surface, aircraft, and satellite platforms. The wavelengths that are most sensitive to cloud structure are in the solar spectrum, yet solar wavelengths are also capable of yielding much information about clouds and constitute numerous datasets. The majority of the problems are associated with side illumination, shadowing, and radiative smoothing via multiple scattering (Marshak et al. 1995). Moreover, the fact that radiative transfer is a nonlinear function of τ means that inferences of τ for medium to large domains are biased systematically (cf., Jensen's inequality).

Great strides have been made in the use of surface-based active cloud sensors such as cloud-profiling radar and lidar though they too have limitations. Notable experiments include the Atmospheric Radiation Measurement (ARM) program (Stokes and Schwartz 1994) and the BALTEX Bridge Campaign (BBC). Combinations of active and passive sensors hold much promise for the future of cloud observations. Research aircrafts are now being outfitted with such configurations (per. comm., J. W. Strapp 2001) as are satellites such as NASA's CloudSat (Stephens et al. 2002) and ESA's proposed EarthCARE (ESA 2001).

The second part of this paper addresses some current issues facing remote sensing of cloud with emphasis on problems arising from 3D cloud structure. The third section looks at various techniques that might be used in LSAMs for addressing interactions between unresolved clouds and radiation. The fourth section discusses briefly cloud/radiative feedback analysis, and conclusions are presented in the final section.

2. Remote sensing of cloudy atmospheres

The purpose of this section is to illustrate some problems facing remote sensing of cloud optical properties that arise through the 3D structure of clouds. Given space and time limitations, this section focuses on remote sensing of cloud optical depth at solar wavelengths. The secondary topic deals with cloud radars since these, relatively new, active sensors appear as though they will play a dominant role in characterizing cloud structure.

2.1 Inference of cloud optical depth from satellite data

Cloud optical depth τ is generally inferred from satellite radiances in the visible or near-infrared. This is because there is very little absorption by droplets and other atmospheric constituents and so reflected radiance as a function of τ saturates slowly thereby maximizing the range of inferable τ. Therefore, as with most methods for inferring τ, it is assumed here that only clouds attenuate radiation.

To begin, one requires either an inverse radiative transfer model, precomputed radiances that form a look-up table, or a forward radiative transfer model imbedded in a root-finding algorithm. The first approach can be expected to be generally intractable and the second is what is used operationally because of time constraints and in principle it can be almost as accurate as the third method. An estimate of surface albedo, or better yet a surface bidirectional reflection distribution function (BRDF), is also required.

Before getting to actual inferences of τ, consider the scale dependence of the problem. Clouds are inherently intermittent objects for they exist where conditions happen to be, or have recently been, conducive to maintain condensed water. Thus, the character of a cloud field will depend on the resolution of the radiance sensor (Gabriel et al. 1988). Figure 1 shows a field of τ simulated by a model with horizontal grid-spacing (tantamount to satellite resolution) of 2-km. If a measured radiance I exceeds some threshold (which depends on solar/viewing geometry and surface BRDF), the pixel is deemed to contain cloud. Since clouds are not always black in the infrared (Coakley and Bretherton 1982), one is usually forced to assume that cloudy pixels are filled with cloud. From this it is immediately clear that inferred τ tend to be underestimates while inferred cloud fractions tend to be overestimates.

Figure 1 shows not a retrieval, but simply a coarsening of resolution from 2, to 4, to 40, and finally 100-km. At each step, τ was averaged for all pixels in a collection of pixels; e.g., at the 40-km pixel resolution, if a collection of 1600 2-km pixels contain as few as one cloudy 2-km pixel whose optical depth is τ2-km, the

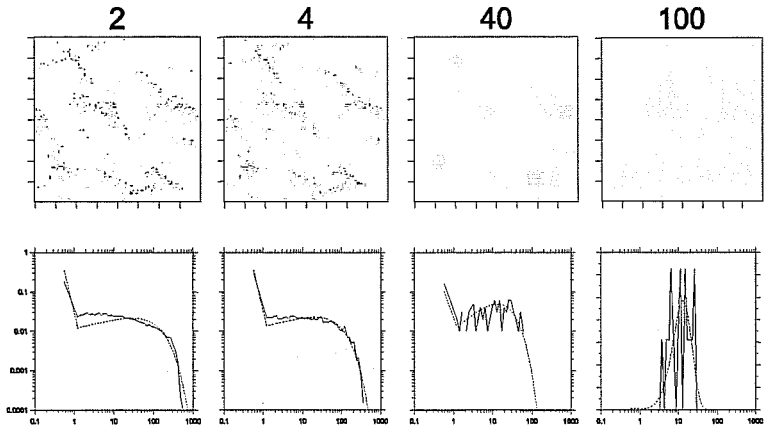

Figure 1. Top row of plots are maps of cloud optical depth τ from a CSM simulation with a domain of 400-km square (Grabowski et al. 1999). Number at top indicates the size of each pixel in kilometres. Inner scale of the model was 2-km. Pixel values of τ were obtained by simply averaging all 2-km pixels (even clear ones) that comprise the larger pixels (i.e., at 40-km, each pixel contained 400 2-km pixels). Lower row of plots are frequency distributions of τ for the corresponding image above (solid lines). Dashed lines are gamma distributions associated with the mean and variance of the observed distributions. Bin widths follow a power law and increase in size as τ increases.

Figure 2 shows how mean $\langle\tau\rangle$, standard deviation of τ, cloud fraction *Ac*, and $\nu = (\langle\tau\rangle/\sigma)2$ vary as functions of resolution. In this case, all quantities are changing rapidly at the 2-km resolution except for ν. This may be important when it comes to parametrizing the interaction of unresolved clouds and radiative transfer in LSAMs. It suggests that future cloud routines that attempt to characterize cloud variability at unresolved scales need aim at a range of scales that is quite broad; in this case it would appear that parametrization at any scale less than ~5-km would be sufficient. Work in this direction is already beginning. Figure 3 shows global distributions of ν derived from ISCCP D1 data which used τ inferred at 5-km for 250-km domains (Rossow et al. 2002). ν was defined for each domain and averaged over time. If clouds behave as those in Fig. 2, and there is absolutely no guarantee they do, this would suggest that distributions of ν shown in Fig. 3 may be representative of what a cloud diagnostic scheme in an LSAM

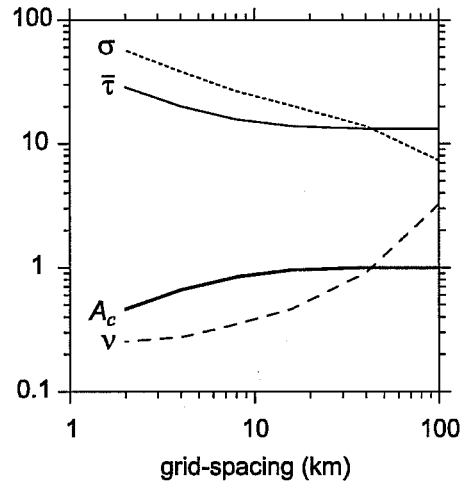

Figure 2. Cloud fraction Ac, mean optical depth $\langle\tau\rangle$, standard deviation σ of τ, and $\nu = (\langle\tau\rangle/\sigma)2$ as functions of horizontal averaging scale for the images shown in Fig. 1.

might aim to achieve. If so, this would imply that the impact of neglecting unresolved interactions between clouds and radiation in LSAMs is large (as will be seen later).

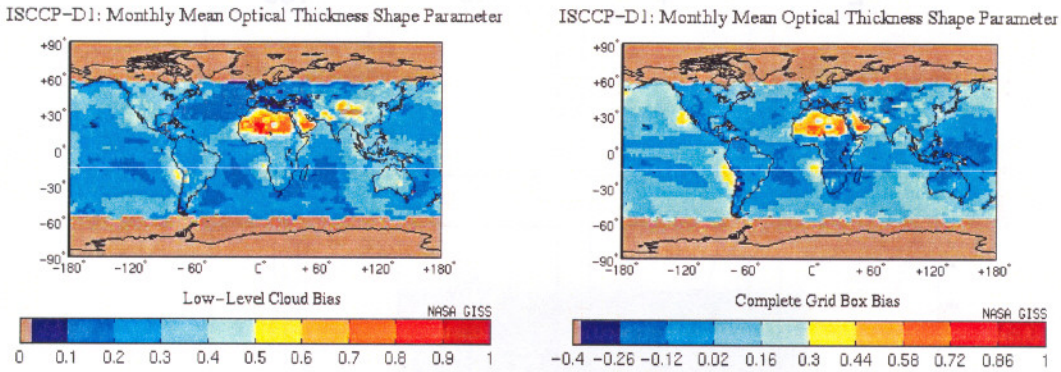

Figure 3. Mean annual, global distributions of log10ν where ν is defined as in the caption of Fig. 2 for low clouds (left panel) and all clouds (right panel) as deduced from ISCCP-D1 data (per. comm., W. B. Rossow 2001).

Figure 4 shows an example of τ inferred from radiances simulated by a 3D Monte Carlo algorithm acting on data produced by a cloud-system model (CSM). The field could be characterized as mostly cloudy with a moderately textured top. A thin, aerosol of optical depth 0.2 was mixed uniformly beneath cloudtop, and the surface had an albedo of 0.092. At θ0 = 30o, retrieval of τ is quite good with most of the error in the form of random error. By θ0 = 60o, however, the error in retrieved τ has blossomed with extreme overestimates for illuminated cloudsides followed by corresponding underestimates for shadowed cloud. This type of error is likely to plague all schemes that employ radiances at few spectral values. Somewhat more success has been demonstrated with high spectral resolution radiances in the oxygen A-band, but this is beyond the scope of this report (per. comm., P. Gabriel 2001).

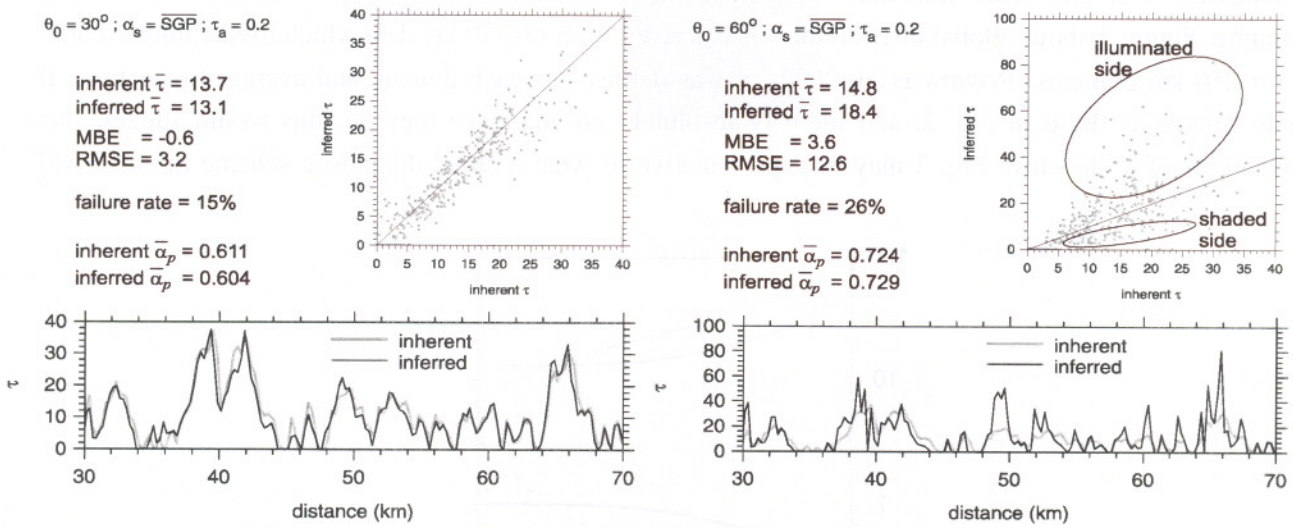

Figure 4. Two sets of inferred optical depth plotted against inherent optical depth for nadir viewing radiances simulated by a 3D Monte Carlo algorithm acting on 2D CSM data. On the left and right respectively are results for solar zenith angles of 30° and 60°. Listed are mean inherent and inferred values of τ as well as mean bias error (MBE) and root mean square error (RMSE). Failure rates are the percentage of cases where radiances were too low to infer a value of τ given the correct underlying surface albedo of 0.092. αp values are domain averaged TOA albedos based on ICA estimates using inherent and inferred distributions of τ. Lower plots show series of inherent and inferred τ for a 40-km stretch of the 100-km domain.

2.2 Inference of cloud optical depth from surface and aircraft data

Compared to satellite, relatively few attempts have been made to infer τ from the surface or aircraft. The most common method for inferring τ from the surface is to use broadband irradiances measured typically by a single pyranometer coupled with estimates of spectral surface albedo (e.g., Leontyeva and Stamnes 1994; Barker et al. 1998). Pyranometers, however, respond to the entire hemisphere so their use for inferring τ is limited to overcast conditions only. Moreover, one can retrieve only *effective* values of τ averaged over the hemisphere.

Given the paucity of reported attempts, it is probably safe to say that there is not a typical method for retrieving τ from aircraft data. The few that have been reported apply to planar clouds and tend to follow something like: by *porpoising* the aircraft from cloudtop to cloudbase, an estimated profile of mean extinction coefficient β is obtained; integrating the profile of β from base to top yields an estimate of $<\tau>$. If the cloud is particularly planar, one my wish to venture an estimate of a time series of τ by multiplying measured β along a transect by the estimated cloud thickness (Gultepe et al. 1999).

Motivated by the restriction on inference of τ from surface and aircrafts to overcast, planar conditions, and a study by Marshak et al. (2000), Barker and Marshak (2001) and Barker et al. (2002a) devised methods that apply well to broken clouds. On account of the novelty of their methods, and the increase in applicable conditions, their method is discussed here in some detail.

Consider spectral downwelling zenith radiance measured by an aircraft-mounted radiometer at point r_0 and altitude z. Knyazikhan and Marshak (2000) and Barker et al. (2002a) showed that this radiance can be expressed as

$$I^{\downarrow}(r_0;z) = I_0^{\downarrow}(r_0;z) + \int_{\Re} F^{\uparrow}(r;z)\, \mathcal{G}(r,r_0;z)dr \tag{1}$$

where $I_0^{\downarrow}$ consists of photons that have not gone below z, $F^{\uparrow}$ is upwelling flux at (r,z), and $\mathcal{G}$ is a radiative Green's function that describes the transfer of $F^{\uparrow}(r,z)$ into $I^{\downarrow}(r_0,z)$. In general, $I_o^{\downarrow}$ can be expected to be an extremely complicated, non-analytic function of τ.

Assuming that clouds transport radiation locally like a 1D medium, define cloudbase reflectance into nadir for upwelling isotropic irradiance as

$$\rho(z) = \int_{\Re} \mathbb{G}(r;z)dr, \tag{2}$$

where $\mathbb{G}$ is similar to $\mathcal{G}$ except it is for isotropic irradiance and homogeneous cloud. Note also that (2) links 1D theory to 3D transfer. Defining a normalized Green's function as

$$\mathcal{H}(r,r_0;z) = \frac{\mathcal{G}(r,r_0;z)}{\int_{\Re} \mathcal{G}(r',r_0;z)dr'} \tag{3}$$

assume that measurements of $F^{\uparrow}(r,z)$ and $I^{\downarrow}(r_0,z)$ are made at two wavelengths $\lambda 1$ and $\lambda 2$ where: 1) atmospheric optical properties above z are very similar, but 2) optical properties of the Earth-atmosphere system below z are very different. Therefore, (2) and (3) can be used in (1) which can be rearranged to solve for (spectrally independent) cloudbase reflectance as

$$\rho(\tau(r_0;z)) \approx \frac{I^{\downarrow}_{\lambda_2}(r_0;z) - I^{\downarrow}_{\lambda_1}(r_0;z)}{\int_{\mathcal{R}} [F^{\uparrow}_{\lambda_2}(r;z) - F^{\uparrow}_{\lambda_1}(r;z)]\mathcal{H}(r,r_0;z)dr}, \tag{4}$$

where the next step is to solve for τ using a tractable 1D model, like DISORT (Stamnes et al. 1988), in a root-finding routine. Note that the offending quantity, $I^{\downarrow}_0$ has been eliminated.

Ideal wavelengths λ to make these measurements are roughly 0.65 μm and 0.85 μm for surface albedos at the former are often much smaller than those at the latter but atmospheric optical properties are almost the same at both λ. This, in essence, isolates photons reflected by the surface. Figure 5 shows an example of how well this method works when surface albedos are 0.092 and 0.381. First, $\mathcal{H}$ is approximated by a delta function (neglecting horizontal transport entirely). This yields initial estimates of τ. The procedure is then rerun using $\mathcal{H}$ portrayed as a gamma distribution (Davis et al. 1997) whose parameters are set by the initial set of τ. In the example shown, the improvement can be significant. There is nothing stopping this procedure from being applied to data collected at a surface site. One would, however, need estimates of local effective surface albedos and time series of spectral downwelling flux and zenith radiance. Likewise, the method should work well for radiometric data obtained on tall meteorological towers.

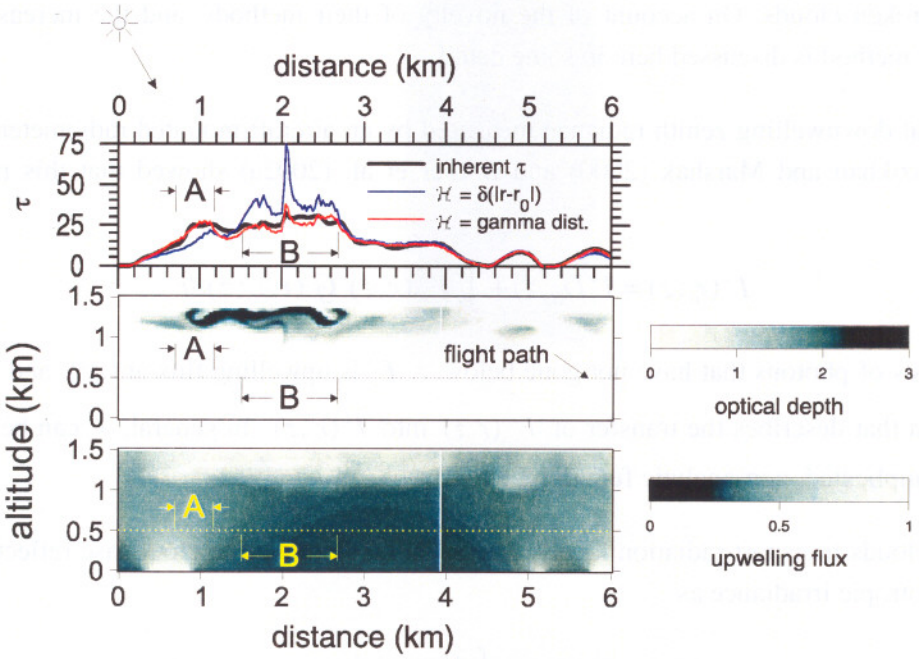

Figure 5. Middle panel shows a 6 km stretch of cloud optical depth τ in each (50 m)2 cell as produced by a 2D CSM. Top panel shows vertically integrated τ (black line) as well as τ inferred assuming that $\mathcal{H}$ is a delta function (blue line) for data collected along the flight path *as indicated in the middle panel. When these inferred values of τ are used to set parameters in a gamma distribution representation of $\mathcal{H}$, the initial estimates are refined and shown as the red line. The lower panel shows upwelling flux at 0.85 μm. The refined estimates of τ are much better in regions A and B because time series of measured upwelling fluxes were used and the algorithm was informed of the dark area to the right of A and likewise the bright area to the left of B. When $\mathcal{H}$ is represented by the delta function, it knows nothing about the horizontal structure of upwelling flux and so estimates of upwelling flux at cloudbase, directly above the aircraft, are poor.*

2.3 What cloud radars give and what LSAMs require

It has been recognized for sometime now that remote sensing of cloud properties using only passive radiances is inherently limited and that significant progress will only be made if active sensors are brought

into play. One of the most promising instruments is the cloud-profiling radar (CPR). The CPR emits pulses of electromagnetic radiation that are reflected by particles in proportion to the sixth power of their radius. Hence, CPRs are quite sensitive to large cloud droplets, but have difficulty sensing small droplets (per. comm., E. E. Clothiaux 2001). As such, inferences of t from passive measurements (or another active sensor like a lidar) are required that respond in proportion to the second power of a particle's radius.

CPRs suffer from the same sampling issues as methods of inferring τ from radiances made on a plane, satellite, or at the surface. Astin et al. (2001) have shown that in broken cloud conditions, transects may have to be several hundred kilometres long before significant reductions can be realized in the confidence intervals for estimates of cloud fraction of the domain from which the transect was drawn. Moreover, Fig. 6 tries to illustrate the situation one will encounter with both CPRs fixed on the surface (as this one is) or on an aircraft or satellite. What is shown is the 512-km domain of a CSM which is taken here to be a grid-cell of a GCM. What the GCM (or the CSM) requires is a time series of the domain. What the CPR (fixed here at 411-km across the domain) gives is a time series of cloud that drifts over it (a satellite might provide the entire domain but only for a single snapshot). As seen in Fig. 6, the time series of cloud obtained at 411-km appears to contain only a slim semblance of the domains. This makes it potentially difficult to compare simulations by NWP and GCMs with particular samples from a CPR.

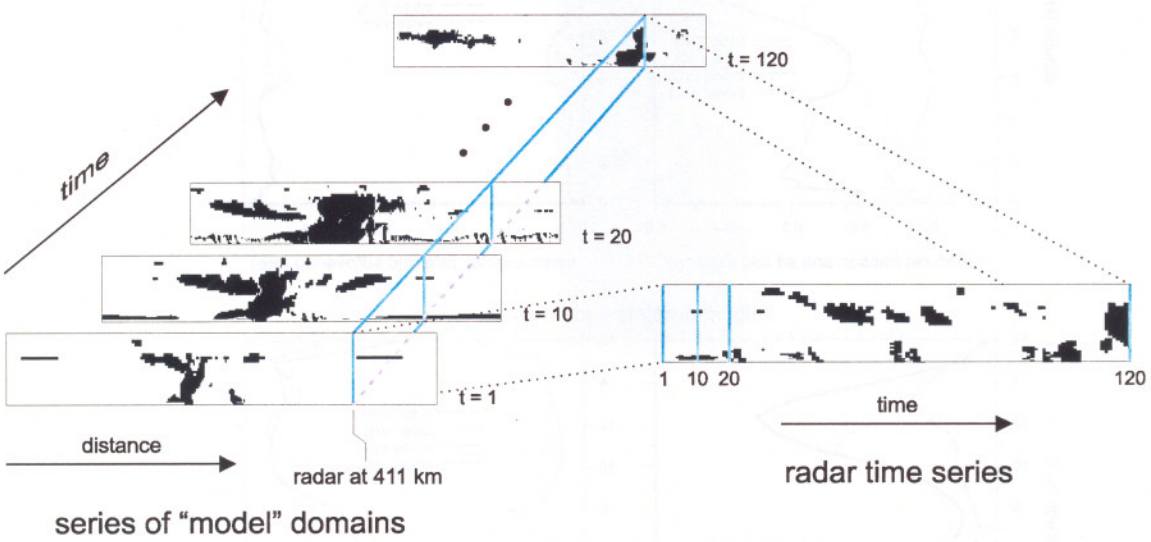

Figure 6. On the right is a sampled time series of cloud masks for a 512-km domain produced by a CSM (Fu et al. 1995). Imagine that a surface-based CPR is fixed at 411-km along the domain. Stringing together the 120 snapshots leads to the domain shown on the right. A GCM or NWP model would want what is on the left, but the radar produced what is on the right. Clearly, in this case, what the radar offers is a rather poor representation of the sequence of domains.

The top panels in Fig. 7 show time-averaged cloud fraction C and fractional cloud overlap Θ in adjacent layers for both the domains associated with Fig. 6 (i.e., what the GCM would have required or simulated and all possible transects obtained by fixed CPRs). These plots correspond to all condensates (liquid droplets, ice crystals, rain, snow, and graupel). Note that both samplings yield identical profiles of expected cloud fraction C (since all pixels were sampled), but the standard deviation of C is generally larger for radar sampling. The upshot is that there is a fairly large probability of drawing a sample with a CPR that is unrepresentative of the time-averaged domain. This, however, does not hold for Θ for it is seen that, in this case, the standard deviation for all possible CPR transects is very similar to that for the domain average.

The lower panels in Fig. 7 are like the uppers except only liquid droplets and ice crystals are considered. This is because these are the condensates that interact most with radiation at wavelengths that are climatologically important (the CPR senses the other constituents better but, due to their size, their influence on climatological radiation budgets is minor). While the same conclusions can be drawn for this case and the case for all constituents, the main difference is not only in C, as could have been expected (smaller C when some hydrometeors are neglected), but Θ are significantly smaller. This is because precipitation imparts a strong maximal overlap signal; once removed, the overlap for cloud exhibits a more pronounced random component. This is understandable given shearing coupled with the spectrum of cloud lifecycles expected over 512-km. The important point here is that when one appeals to CPR data to construct parametrizations of cloud overlap (e.g., Hogan and Illingworth 2000), the maximal overlap signal of precipitation will skew one's impression, and subsequent impact, of cloud overlap (not only for radiation, but for other processes too).

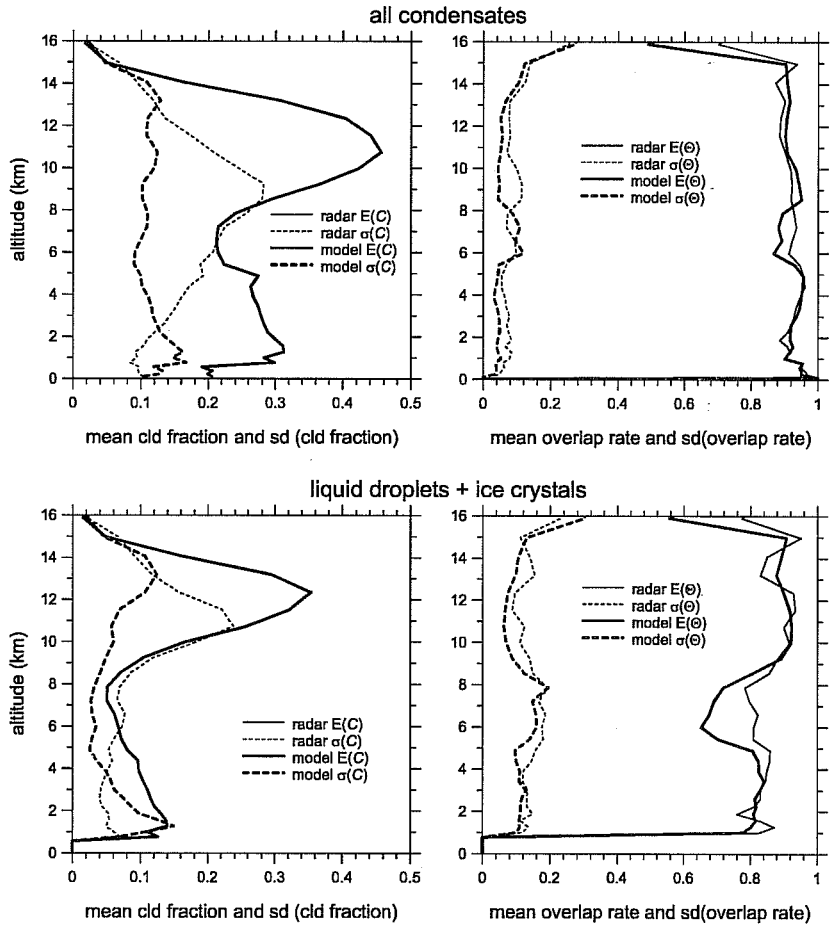

Figure 7. Top left panel shows the expectation E profiles of cloud fraction C produced by averaging across all domains in Fig.6 using all condensates. This profile is the same as that expected from all possible radar time series. The standard deviation σ of these profiles obtained from all domain profiles is, however, usually much smaller than σ for all possible radar series. The upper right panel is similar to the upper left except it is for E and σ for profiles of adjacent overlap fraction Θ. Lower panels are like the upper panels except they correspond to only liquid droplets and ice crystals (i.e., large hydrometeors are neglected).

3. Accounting for unresolved cloud and radiation in LSAMs

The purpose of this section is to discuss, briefly, some methods that could be used in LSAMs to account for interactions between unresolved clouds and radiation. Some outstanding issues facing both solar and terrestrial radiation are discussed as well.

3.1 Solar radiation

Many studies (already cited) have examined the scale dependent interactions between variable clouds and SW radiative transfer. Several methods of accounting for unresolved cloud effects on mean transport properties are reviewed briefly. This is not an exhaustive review.

One of the first ways of addressing unresolved cloud effects in a tractable manner was presented by Cahalan et al. (1994). Assume that nonabsorbing PPH cloud albedo as a function of cosine of solar zenith angle $\mu 0$ and τ can be approximated as

$$R_{pp} \approx \frac{\tau}{15\mu_0 + \tau}, \tag{5}$$

which upon expansion in a Taylor series and averaging gives

$$\begin{aligned} \overline{R} &= R_{pp}(\eta\overline{\tau}) + \sum_{n=1}^{\infty} \mathcal{M}_{2n} \frac{\partial^{2n} R_{pp}}{\partial(\ln\tau)^{2n}} \Big| \eta = \frac{e^{\overline{\ln\tau}}}{\overline{\tau}} \\ &\approx R_{pp}(\eta\overline{\tau}) \end{aligned} \tag{6}$$

where $\mathcal{M}_{2n}$ is proportional to the variance of τ. The approximate solution is valid when mean τ is near the inflection point of R_{pp} as a function of $\ln\tau$ (which in this case occurs at $\tau = 15\mu 0$; see Fig. 8), or when $\mathcal{M}_{2n}$ are small (i.e., weak variability). The scaling actor η has been used for years as a blind tuning factor to counter the use of PPH two-stream models. What Cahalan et al. (1994) did was to instill it with a physical meaning.

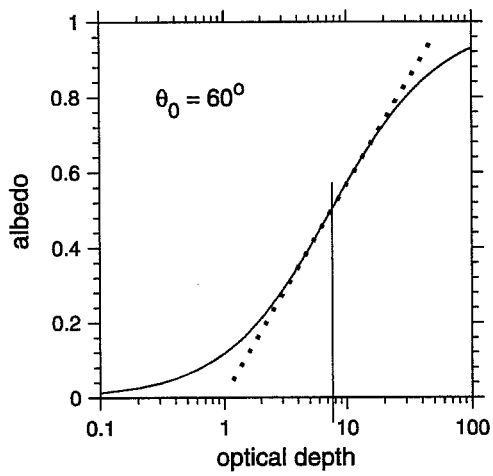

Figure 8. Cloud albedo as described in (5) at a solar zenith angle of 60o as a function of optical depth τ plotted on a log-scale. The inflection point is marked at $\tau = 7.5$ and the dashed line is the corresponding tangent line. For τ close to the inflection point, albedo as a function of logτ is almost linear.

Barker (1996) took more of a brute force approach by defining the distribution of τ as

$$p_\gamma(\tau) = \frac{1}{\Gamma(\nu)}\left(\frac{\nu}{\overline{\tau}}\right)^\nu \tau^{\nu-1} e^{-\nu\tau/\overline{\tau}} \,|\, \tau > 0; \nu > 0, \tag{7}$$

where Γ is the gamma function and ν defines the shape of the gamma distribution. Then, albedo of an inhomogeneous cloud is approximated as (Stephens et al. 1991)

$$\overline{R} = \int_0^\infty p_\gamma(\tau) R_{pp}(\tau) d\tau. \tag{8}$$

Using (7) and the general solutions for the non-conservative two-stream approximation in (8), mean transmittance and albedo can be expressed as

$$\begin{aligned} T_\Gamma &= \left(\frac{\nu}{\nu + \overline{\tau}/\mu_0}\right)^\nu - \phi_1^\nu \frac{\omega_0}{a}\left[t_+ \mathcal{F}(\beta,\nu,\phi_4)\right] - t_- \mathcal{F}(\beta,\nu,\phi_5) - t\mathcal{F}(\beta,\nu,\phi_6) \\ R_\Gamma &= \phi_1^\nu \frac{\omega_0}{a}\left[r_+ \mathcal{F}(\beta,\nu,\phi_1) - r_- \mathcal{F}(\beta,\nu,\phi_2) - r\mathcal{F}(\beta,\nu,\phi_3)\right] \end{aligned} \tag{9}$$

where

$$\mathcal{F}(\beta,\nu,\phi) = \sum_{n=0}^{\infty} \frac{\beta^n}{(\phi+n)^\nu}; \left[|\beta| \le 1, \beta \ne 1, \nu > 0\right] \tag{10}$$

in which the definition of most terms can be found in Eq.10 of *An Overview of Methods for Handling, and Issues Facing, Sub-grid-scale Radiative Transfer in Large-scale Atmospheric Models* in this volume. The only terms not defined there are ϕi which depend on cloud optical properties and $\mu 0$. This method is referred to hereinafter as the gamma-weighted two-stream approximation (GWTSA).

Stephens (1988) proposed a method for solving the 1D radiative transfer equation which assumes that

$$\overline{\beta' I'} = C_{\beta I}\,\overline{\beta I} = f_\beta f_I r_{\beta I} \mu, \tag{11}$$

where fluctuations in intensity I' and extinction β' are correlated by a amount r_{β_I} and depend linearly on zenith angle μ. This results in the regular two-stream expressions for albedo and transmittance, but β and single-scattering albedo $\omega 0$ are replaced by

$$\begin{aligned} \tilde{\beta} &= (1 + C_{\beta I})\overline{\beta} \\ \tilde{\omega}_0 &= \left[\frac{1 + C_{SI}}{1 + C_{\beta I}}\right]\omega_0 \end{aligned} \tag{12}$$

where C_{β_I} and C_{SI} describe correlations between intensity and total extinction and scattering extinction, respectively.

In a similar manner, Cairns et al. (1999) derived expressions for two-stream albedo and transmittance for a cloud that possesses small-scale 3D variability. This results in

$$\left.\begin{aligned}\tilde{\beta} &= \frac{\overline{\beta}}{1+\nu} \\ \tilde{\omega}_0 &= \frac{\omega_0}{1+\nu(1-\omega_0)} \\ \tilde{g} &= g\frac{1+\nu(1-\omega_0)}{1+\nu(1-\omega_0 g)}\end{aligned}\right\} \nu = \left(\frac{\sigma_N}{N}\right)^2 = \frac{1}{\nu} \tag{13}$$

where g is asymmetry parameter, N is droplet concentration, and σ_N is standard deviation of droplet concentration. Figure 9 shows cloud albedo and absorptance as functions of mean optical depth for the standard PPH model, Cairns et al.'s model, and the GWTSA. Single-scattering albedo is fairly small at 0.999, so absorptance is moderate, and variability is moderate too with n = = 1. From this plot, it is clear that Cairns et al.'s ν model is not intended to capture large-scale variability for it deviates only slightly from the PPH solution. An interesting idea might be to merge Cairns et al.'s model with the GWTSA.

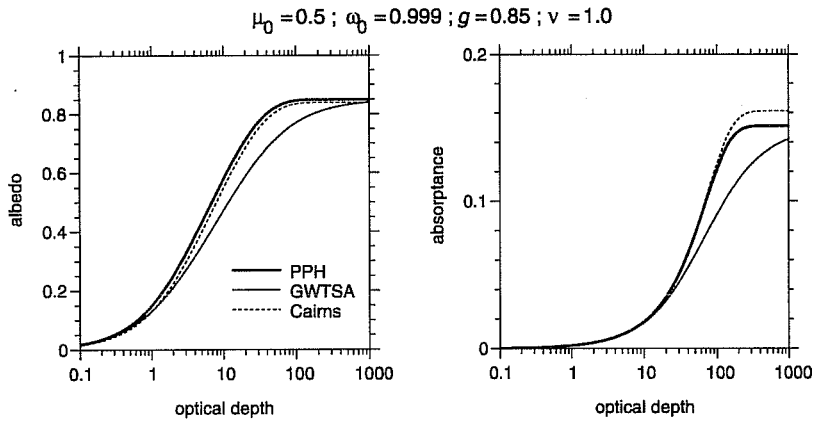

Figure 9. Cloud albedo and absorptance as functions of optical depth for the regular two-stream model (PPH), Cairns et al.'s model, and the GWTSA for conditions listed at the top of the plots. The underlying surface was black.

Thus far, only single layer clouds have been discussed. In general, one can expect *a cloud field* as simulated by an NWP model or GCM to span several arbitrary layers. This poses a problem since fluxes inside a horizontally variable cloud, unlike those inside a homogeneous cloud, also vary horizontally. Since the two-stream solution accounts only for mean fluxes at model levels, one cannot link layers following the straightforward adding process.

Consider the simple case of normal incident direct-beam onto a cloud that is variable in the horizontal but vertically homogeneous. If the variability is defined using (7), then mean direct-beam transmittance is defined as

$$\overline{T} = \int_o^\infty p_\gamma(\tau) e^{-\tau} d\tau = \left(\frac{\nu}{\nu+\overline{\tau}}\right)^\nu. \tag{14}$$

If the cloud is now partitioned into N equal layers and mean transmittance is computed for each layer as in (14) and the N values are multiplied together, as would be done in a homogeneous two-stream model, mean transmittance is defined as

$$\lim_{N\to\infty}\left[\prod_{k=1}^{N}\left(\frac{\nu}{\nu+\tilde{\tau}/N}\right)^{\nu}\right]=N(\text{or }\nu)\overset{\lim}{\to}\infty\left[\left(\frac{\nu N}{\nu N+\tilde{\tau}}\right)^{\nu N}\right]=e^{-\overline{\tau}} \tag{15}$$

From this it can be seen that the number of layers N and ν are interchangeable. So, just as ν going to infinity implies homogeneity, so too does N going to infinity when the conventional method of multiplying layer mean transmittances is applied (i.e., Beer's law is recovered).

Oreopoulos and Barker (1999) circumvented this problem by renormalizing the distribution of τ for each layer and defining a downward reduced mean τ (following the main stream of radiation) in each layer of a contiguous block of cloudy layers as

$$\begin{cases}\overline{\tau}_2^{*}=\dfrac{\nu\overline{\tau}_2}{\nu+\overline{\tau}_1}\le\overline{\tau}_2\\ \quad\vdots\\ \overline{\tau}_N^{*}=\dfrac{\nu\overline{\tau}_N}{\nu+\sum_{j=1}^{N-1}\overline{\tau}_j}\le\overline{\tau}_N\end{cases} \tag{16}$$

Note that the uppermost layer in unaltered as it is assumed that incident radiation is homogeneous (this goes for either the absolute uppermost cloud and clouds beneath the uppermost cloud that are separated from one another by a cloudless gap).

While this adjustment is strictly applicable to direct-beam only, Oreopoulos and Barker applied it to scattered radiation too, though in a highly parametrized fashion.

3.2 Terrestrial radiation

All discussions here regarding interactions between unresolved clouds and terrestrial (LW) radiation involve the 1D code developed by Li (2002) (see the companion paper to this one) and Li and Barker (2002).

First, recall that Li (2002) defined flux at the base of the jth layer as

$$F_j^{-}=F_{j-1}^{-}e^{-\langle\kappa\rangle_{j-1}/\mu_1}+\tilde{\beta}_{j-1+1/2}\left(1-e^{-\langle\kappa\rangle_{j-1/\mu_1}}\right) \tag{17}$$

where $\mu_1 = 0.601$ (Li 1999), $B' = \pi B$, where B is the Planck function, and

$$\langle\kappa\rangle_j=(1-\omega_0)\tau_j \tag{18}$$

is absorption optical depth for the jth layer. For an inhomogeneous layer with uniform irradiance, however, (17) is

$$F_j^{-}=F_{j-1}^{-}\tau\left(\langle\kappa\rangle_{j-1},\nu_{j-1}\right)+\tilde{B}_{j-1+1/2}\left[1-\tau\left(\langle\kappa\rangle_{j-1},\nu_{j-1}\right)\right], \tag{19}$$

and if (7) is used to represent cloud variability,

$$\tau\left(\langle\kappa\rangle_{j-1},\nu_{j-1}\right)=\int_0^{\infty}p_\gamma(\kappa|\langle\kappa\rangle_{j-1},\nu_{j-1})e^{-\kappa/\mu_1}d\kappa=\left(\frac{\nu_{j-1}}{\nu_{j-1}+\langle\kappa\rangle_{j-1}/\mu_1}\right)^{\nu_{j-1}} \tag{20}$$

If this was applied to each layer and layers linked as though the clouds were homogeneous, then from the discussion at the end of the previous section, this would lead to terms like

$$\tau\left(\langle\kappa\rangle_{j-1},\nu_{j-1}\right)\tau\left(\langle\kappa\rangle_{j-2},\nu_{j-2}\right), \tag{21}$$

when what are sought are terms like

$$\tau\left(\langle\kappa\rangle_{j-1}+\langle\kappa\rangle_{j-2},\nu_{j-2,j}\right)=\tau\left(\langle\kappa\rangle_{j-2,j},\nu_{j-2,j}\right),\langle\kappa\rangle_{k,j}=\sum_{m=j-1}^{k}\langle\kappa\rangle_{m} \tag{22}$$

where $\nu_{j-2,j}$ corresponds to the variance of τ for the collection of (in this case two) layers.

Thus, expanding (19) as in (18) in the companion paper, mean flux emerging from the base of the *j*th layer is

$$\begin{aligned}F_j^- =&\left(F_{i-n}^- -\tilde{B}_{i-n+1/2}\right)\tau\left(\langle\kappa\rangle_{i-n,j},\nu_{i-n,j}\right)\\ &+\left(\tilde{B}_{i-n+1/2}-\tilde{B}_{i-n+1+1/2}\right)\tau\left(\langle\kappa\rangle_{i-n+1,j},\nu_{i-n+1,j}\right)\\ &+\cdots+\left(\tilde{B}_{j-3+1/2}-\tilde{B}_{j-2+1/2}\right)\tau\left(\langle\kappa\rangle_{j-2,j},\nu_{j-2,j}\right)\\ &+\left(\tilde{B}_{j-2+1/2}-\tilde{B}_{j-1+1/2}\right)\tau\left(\langle\kappa\rangle_{j-1,j},\nu_{j-1,j}\right)\\ &+\tilde{B}_{j-1+1/2}.\end{aligned} \tag{23}$$

The complexity that this entails is illustrated in Fig. 10. Not only is ν for each layer required, which at present is a tall order, but ν for collections of all cloudy layers in a contiguous block of clouds are required too. This entire procedure can be enhanced to include nonconstant Planck functions across layers (important for geometrically thick layers), scattering by hydrometeors, and cloud overlap. Discussion of these aspects is too detailed for this venue; interested readers can refer to Li and Barker (2002).

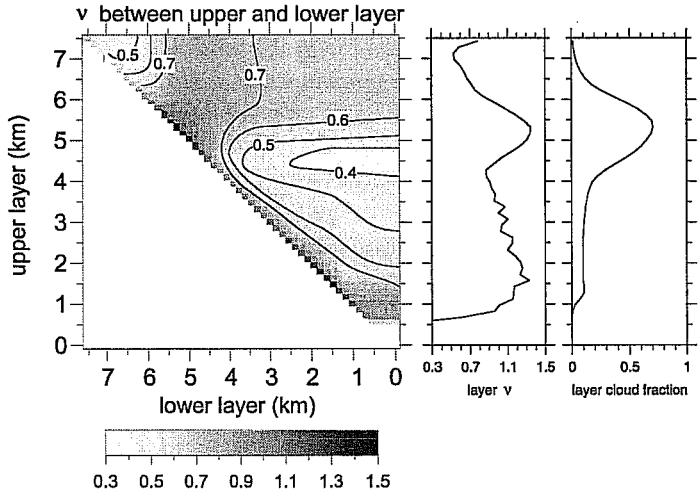

Figure 10. Plots on the right show profiles of cloud fraction and ν [as defined in (7)] for a 3D field of clouds simulated by a CSM (Anderson et al. 1997). Panel on the left shows ν for collections of layers between a lower *altitude and an* upper *altitude. Values of ν for each layer (i.e., the profile on the right) are along the main diagonal. Note that for the collective cloud between cloudbase (at ~0.7 km) and 5 km, ν is as small as 0.39 which is much less than any single layer value. This is due to a mix of random and maximum overlap of cloud. Likewise, ν for the entire depth of cloud is ~0.65.*

Figure 11 documents an interesting counterintuitive outcome of interactions between variable cloud and LW radiation. The left panel in Fig. 11 shows heating rate as a function of altitude and mean ice water content *IWC* (vertically homogeneous cloud) for a cirrus cloud with horizontal variability defined by a gamma distribution. The right panel shows differences in heating rate for a corresponding PPH cloud with the same mean *IWC* as the inhomogeneous cloud and the inhomogeneous heating rates. The interesting point here is that PPH clouds cool less from their tops when mean *IWC* is < 0.01 g m-3 whereas for denser clouds, the tops of PPH clouds cool more. This may seem counterintuitive but it can be explained by noting that the uppermost layer's cooling rate for PPH cloud is a concave-down function of *IWC* for very small *IWC* and concave-up for larger *IWC*. Hence, using Jensen's integral inequality, it is clear that depending on the extent of horizontal variability (as well as other cloud and atmospheric properties), there will be a reversal in the sign of PPH heating anomaly at some mean *IWC*.

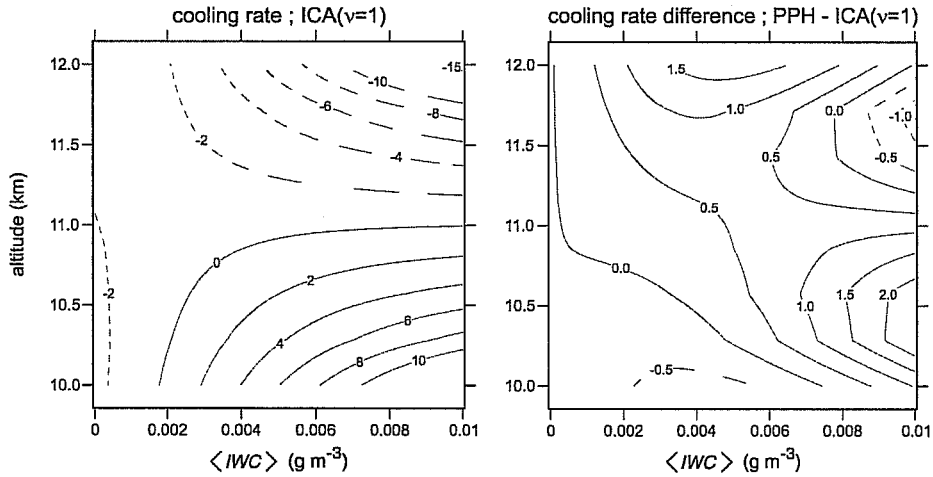

Figure 11. Plot on the left shows domain averaged cooling rate (K/day) profiles through a horizontally inhomogeneous cirrus cloud (characterized by v = 1) situated between 10 and 12 km as a function of mean ice water content IWC (cloud is vertically homogeneous). As mean IWC increases, the cloud becomes blacker and cools more from it top while its base warms due to absorption of radiation emitted by the warmer underlying surface-atmosphere system. Plot on the right shows differences in domain averaged cooling rates produced by the inhomogeneous cloud (as shown on the left) and the corresponding plane-parallel, homogeneous (PPH) cloud with the same mean IWC. Note that for small IWC, the top of the PPH cloud cools less than does the inhomogeneous cloud. This counterintuitive result is reversed at larger mean IWC. See Li and Barker (2002) for an more thorough discussion.

3.3 Radiative forcing due to neglect of unresolved clouds in an LSAM

The dynamical impact of neglecting interactions of clouds and radiation at scales that are unresolved by LSAMs has only started to be explored. In a cursory manner, Tiedtke (1996) considered the SW impact of scaling liquid water path for stratiform clouds in an ECMWF model in a manner like that of Cahalan et al. (1994). Recently, Cole et al. (2002) applied the GWTSA, as discussed in sections 3.1 and 3.2, in diagnostic mode to the Canadian (CCCma) GCM. This was achieved by simply running the GCM using fluxes computed by the GWTSA and on each timestep that saw a full radiation calculation, fluxes were also computed using the regular PPH code. Both sets of calculations used the same cloud fractions, optical properties, and overlap assumptions. Thus, they were able to estimate the *forcing* due to neglect of unresolved cloud/radiation interactions. Their primary results are presented here.

Clouds in this version of the CCCma-GCM are prognostic in the vertical only, and layer cloud fractions *Ac* were diagnosed with a modified version of Xu and Randall's (1996) scheme (per. comm., N. McFarlane 2001). Unresolved fluctuations of cloud were described as

$$\nu = \begin{cases} 1\ ;\ A_c < 0.9 \\ 2\ ;\ 0.9 \le A_c \le 0.99 \\ 4\ ;\ A_c > 0.99 \end{cases} \tag{24}$$

The maps in Fig. 12 show the change in net radiative fluxes at the TOA averaged over five northern summers. These can also be interpreted as changes in TOA cloud radiative forcing (CRF) when going from GWTSA to PPH. While some areas (with persistent low cloud with fractional amounts when present < 0.9) exhibit increases in SW CRF as large as –25 W m^{-2}, most regions display only about –5 W m^{-2}. Likewise, for different regions, especially in the ITCZ where cirrus are abundant, maximum increases in LW CRF are about 10 W m^{-2} but most areas show only about 2 W m^{-2}. These forcings were expected to be somewhat larger but in all likelihood were suppressed for two reasons. First, the maximum-random cloud overlap method was used. This tends to create effectively thick clouds (especially convective cloud) with near saturated albedo regardless of whether cloud inhomogeneity is accounted for or not. Also, by tying estimates of ν to A_c when present, the impact of subgrid-scale variability is at the mercy of a good parametrization of A_c. It is suspected that for the effective grid-spacing used in this version of the GCM, there are too many occurrences of very small values of A_c and values of A_c near 1. As such, the impact of neglecting unresolved fluctuations of cloud are squelched. Obviously, more physically consistent scheme for setting ν is much needed.

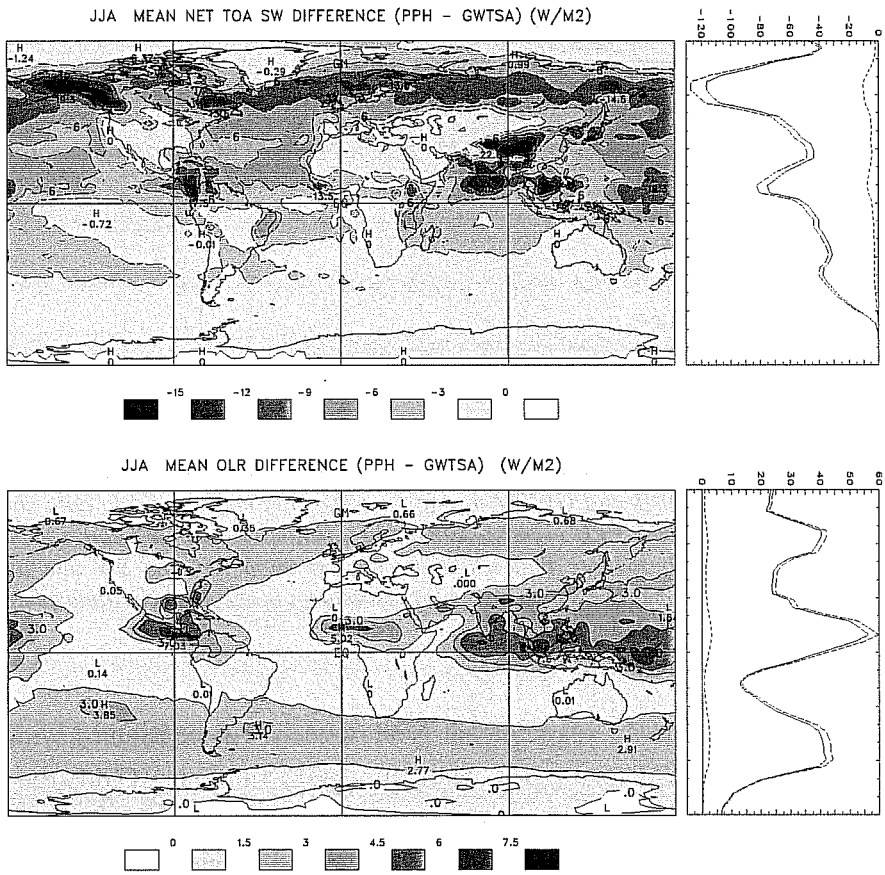

Figure 12. Upper map shows difference between northern hemisphere summer mean TOA net SW flux (or SW cloud radiative forcing CRF*) (W m-2) produced by the CCCma-GCM using both plane-parallel, homogeneous (PPH) clouds and clouds with unresolved fluctuations described by (24). Lower map shows corresponding values for OLR (or LW* CRF*). Plots on the right show zonal mean values of* CRF *for both radiation codes as well as differences (negative differences for the SW and positive differences for the LW indicate that PPH clouds reflect more and allow less OLR, respectively.*

Figure 13 shows zonal-average cross sections of SW and LW heating rates corresponding to Fig. 12. For the SW the overwhelming effect is slightly more heating by PPH clouds. Beneath thick (or persistent) clouds, absorption by water vapour is reduced for the PPH clouds due to decreased transmittance. For the LW, the PPH clouds cool more from their tops and less from their bases. This is clear for all three areas of abundant cirrus.

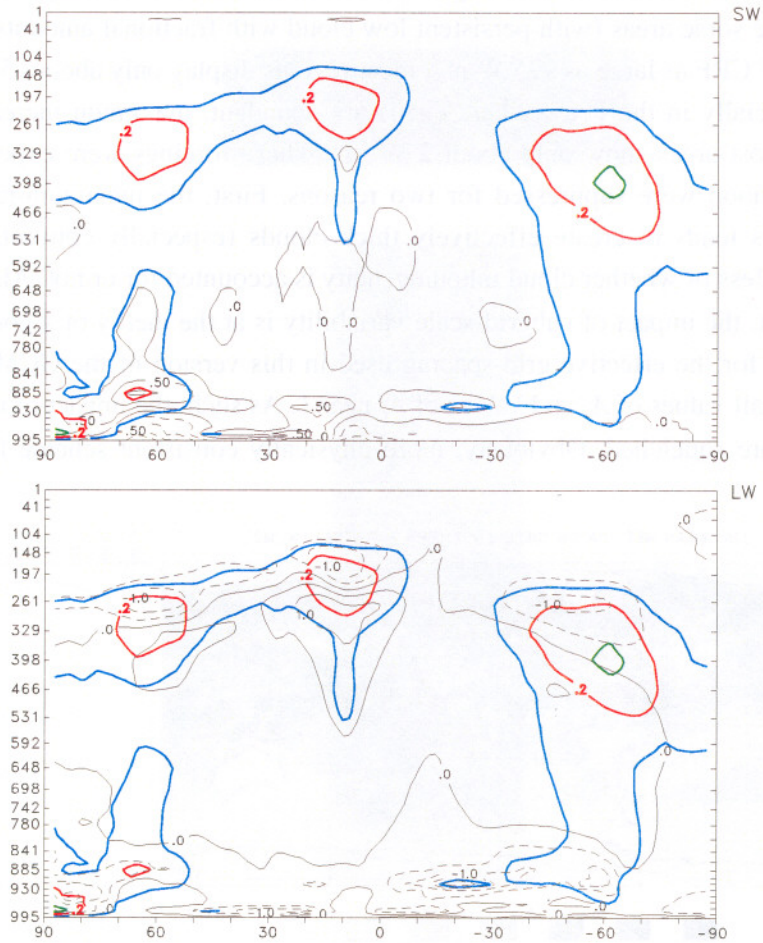

Figure 13. Black lines indicate zonally averaged cross sections of differences between SW and LW heating rates predicted by the PPH and GWTSA radiation codes and correspond to data shown in Fig. 12. Positive values indicate that the PPH clouds absorb more. Coloured lines indicate zonally averaged cloud fractions. It is interesting to note that while the largest impact in the SW due to neglect of unresolved clouds is on TOA (and surface) fluxes, the largest impact in the LW is in atmospheric heating.

3.4 High-spatial resolution strategies

It is likely that within the next 10 to 15 years, global NWP models will be running with horizontal grid-spacing Δx on the order of 10 km (per. comm., J.-J. Morcrette 2001). Currently, CSMs run with Δx between 2 km and 5 m. In light of this, it seems reasonable to ask: is it necessary to execute radiative transfer codes at every column? While at such small Δx the assumption of homogeneous clouds will in many cases be a fair approximation, net radiative fluxes out the sides of columns will often be in serious violation. These considerations aside, is it necessary that radiative heating be resolved at the small scale Δx or need it be resolved only at a scale $\Delta x >> \Delta x$ provided mean flux profiles at Δx are accurate?

An affirmative answer to this question could save CSMs and high-resolution NWP models substantial amounts of CPU time. The idea would be that much cloud information is resolved at Δx and could be used to

to initialize a reliable 1D model that could handle descriptions of unresolved cloud structure (i.e., overlap and horizontal variability). It remains, however, to be shown how large ΔX can be and under what conditions can it be maximized without imparting adverse effects on the evolution of the system. At present, experiments addressing this question have begun with CSMs.

4. Analysis of cloud-radiative feedbacks

Assume that over a sufficiently long time period Earth is in radiative equilibrium at the TOA and that equilibrium is perturbed by an amount ΔR. Allowing Earth to recover its equilibrium, the resulting change in mean surface temperature ΔTs can be approximated using linear feedback theory as (e.g., Schlesinger and Mitchell 1987)

$$\Delta T_s \approx \frac{-\Delta R}{\underbrace{\frac{\partial \mathcal{I}}{\partial T_s} + \frac{S_\odot}{4}\frac{\partial \alpha_p}{\partial T_s}}_{\text{initial}} + \underbrace{\underbrace{\sum_i \left[\frac{\partial \mathcal{I}}{\partial x_i} + \frac{S_\odot}{4}\frac{\partial \alpha_p}{\partial x_i}\right]}_{\text{radiative}} \underbrace{\frac{dx_i}{dT_s}}_{\text{dynamic}}}_{\text{feedbacks}}}, \tag{25}$$

where $\mathcal{I}$ is outgoing LW radiation, $S_\odot$ is the solar constant, αp is TOA albedo, and x_i are climatic variables. The term labeled *initial* accounts for the recovery in the absence of feedbacks. The term labeled *feedbacks* allows for changes to clouds, water vapour, surface albedo etc. during Earth's attempt to recover equilibrium.

Normally, discussions of cloud-radiative feedbacks address variables such as cloud fraction, cloudtop altitude, and mean optical depth to name a few. What if, however, subgrid-scale variable clouds are acknowledged? Is it reasonable to expect a feedback term that looks like

$$\frac{\partial \alpha_p}{\partial \nu}\frac{d\nu}{dT_s} \tag{26}$$

where ν is from (7)? How should such an expression be interpreted? It seems unreasonable to assume that the geometric structure of each cloud would change, but it seems less unreasonable to assume that the geometric structure of cloud fields might change under a climatic change (e.g., size and spacing distribution of clouds). Perhaps even more reasonably, it could also be viewed as simply changing frequency of occurrence of different clouds associated with different meteorological conditions where different cloud types have different distributions of ν?

This last point actually gives rise to a broader definition of climate feedback; it may be that under a climatic change, the mean of a variable might not change, but the variable's underlying distribution might change. This is as much climatic change as mean values changing. Thus, it might be better to envisage a feedback defined, not as in (26), but rather as

$$\int_0^1 \int_0^\infty \left[\frac{\partial \alpha_p}{\partial \nu}\frac{d\nu}{dT_s}\right] p\left(\nu \middle| \alpha_p\right) d\nu d\alpha_p, \tag{27}$$

where $p(\nu|\alpha_p)$ is a normalized conditional frequency distribution of ν given α_p (a more thorough form would involve n-dimensional conditional distributions including both position and time).

Conclusion

The intention of this manuscript was neither to give an exhaustive discussion of all issues nor an exhaustive discussion of any single issue facing radiative transfer for inhomogeneous cloudy atmospheres. Rather, the intention was to provide a sampling of issues from remote sensing, to large-scale modelling, to climate sensitivity where radiative transfer and cloud structure are important and being dealt with at present. In spots it was somewhat speculative and meant to generate thought, while in others it drew on established points and procedures backed by a lineage of studies.

It has been know for some time now that the assumption that clouds are plane-parallel, homogeneous (PPH) media is invalid and can have systematic ramifications on remote retrieval of cloud properties and on the representation of cloud-radiation interactions in LSAMs. In many respects, issues of 3D radiative transfer for inhomogeneous clouds are less tractable with respect to remote sensing than with representation in LSAMs. Indeed, virtually no attempts have been made to account for 3D effects in operational remote sensing algorithms. Thus, this is still a wide-open field with much work still remaining to be done (Varnai and Marshak 2001). Over the next decade the challenge for advancement is even more pressing as expensive multi-agency satellite missions directed squarely at clouds begin to unfold.

There are now several algorithms available for use in LSAMs that attempt to account for both unresolved cloud overlap patterns and horizontal variability. Indeed, results of a recent intercomparison study of 1D codes suggests that the codes are capturing much of what they intend to capture (Barker et al. 2002b). The main issue over the next decade or so will likely not be on improving radiative transfer codes, though some work still remains with respect to multi-layered codes, but rather development of cloud algorithms that are able to diagnose the vertical and horizontal structure of unresolved cloud. The hard reality is that one could have a line-by-line 3D Monte Carlo radiative transfer code in an LSAM and see little improvement in the simulation of weather and climate if the representations of water vapour and cloud water were poor. Thus, it is imperative that cloud routines keep in step with radiation codes and supply them with essential pieces of information that are at present completely lacking.

References

Anderson, W. D., V. Grubisic, and P. K. Smolarkiewicz, 1997: Performance of a massively parallel 3D non-hydrostatic atmospheric fluid model. PDPTA'97 International conference, 645-651.

Astin, I., L. Di Girolamo, and H. M. van de Poll, 2001: Bayesian confidence intervals for true fractional coverage from finite transect measurements: implications for cloud studies from space. *J. Geophys. Res.*, **106**, 17303-17310.

Barker, H. W., 1996: A Parameterization for Computing Grid-Averaged Solar Fluxes for Inhomogeneous Marine Boundary Layer Clouds. Part I: Methodology and homogeneous biases. *J. Atmos. Sci.*, **53**, 2289-2303.

Barker, H. W., T. J. Curtis, E. Leontieva, and K. Stamnes, 1998: Optical depth of overcast cloud across Canada: Estimates based on surface pyranometer and satellite measurements. *J. Climate*, **11**, 2980-2994.

Barker, H. W., G. L. Stephens, and Q. Fu, 1999: The sensitivity of domain-averaged solar fluxes to assumptions about cloud geometry. *Q. J. R. Meteorol. Soc.*, **125**, 2127-2152.

Barker, H. W. and Q. Fu, 2000: Assessment and optimization of the gamma-weighted two-stream approximation. *J. Atmos. Sci.*, **57**, 1181-1188.

Barker, H. W. and A. Marshak, 2001: Inferring Optical Depth of Broken Clouds above Green Vegetation using Surface Solar Radiometric Measurements. *J. Atmos. Sci.*, **58**, 2989–3006.

Barker, H. W., A. Marshak, W. Szyrmer, A. Trishchenko, J.-P. Blanchet, and Z. Li, 2002a: Inference of Cloud Optical Depth from Aircraft-based Solar Radiometric Measurements. *J. Atmos. Sci.*, **59**, 2093-2111.

Barker, H. W., and others, 2002b: Assessing 1D Atmospheric Solar Radiative Transfer Models: Interpretation and Handling of Unresolved Clouds. Submitted to *J. Geophys. Res.*

Cahalan, R.F., W. Ridgway, W.J. Wiscombe, T. L. Bell, and J.B. Snider, 1994: The albedo of fractal stratocumulus clouds. *J. Atmos. Sci.*, **51**, 2434-2455.

Cairns, B, A. A. Lacis, and B. E. Carlson, 2000: Absorption within inhomogeneous clouds and its parameterization in general circulation models. *J. Atmos. Sci.*, **57**, 700-714.

Coakley, J.A., Jr., and F.P Bretherton, 1982: Cloud cover from high resolution scanner data: Detecting and allowing for partially filled fields of view *J. Geophys. Res.*, **87**, 4917-4932.

Cole, J., H. W. Barker, J. Li, and N. A. McFarlane, 2002: Radiative Forcing by Unresolved Fluctuations in Cloud Water Path in a GCM. Submitted to *J. Climate.*

Davis, A. B., A. Marshak, R. F. Cahalan, and W. J. Wiscombe, 1997: The Landsat scale-break in stratocumulus as a three-dimensional radiative transfer effect: Implications for remote sensing. *J. Atmos. Sci.*, **54**, 241-260.

ESA, 2001: *The Five Candidate Earth Explorer Core Missions*: Reports for Assessment. SP-1257-1.

Fu, Q., S. K. Krueger, and K.-N. Liou, 1995: Interactions of radiation and convection in simulated tropical cloud clusters. *J. Atmos. Sci.*, **52**, 1310-1328.

Gabriel, P., S. Lovejoy, A. Davis, G. Austin, and D. Schertzer, 1988: Multi-fractal analysis of resolution dependence in satellite imagery. *Geophys. Res. Lett.*, **15**, 1373-1376.

Grabowski, W. W., X. Wu, M. W. Moncrieff, and W. D. Hall, 1998: Cloud-resolving modeling of cloud systems during phase III of GATE. Part II: Effects of resolution and the third spatial dimension. *J. Atmos. Sci.*, **55**, 3264-3282.

Gultepe, I., G. A. Isaac, and K. B. Strawbridge, 2001: Variability of cloud microphysical and optical parameters obtained from aircraft and satellite remote sensing during RACE. *Inter. J. Climate*, **21**, 507-525.

Hogan, R. J. and A. J. Illingworth, 2000: Derived cloud overlap statistics from radar. *Q. J. R. Meteorol. Soc.*, **126**, 2903-2909.

Intergovernmental Panel on Climate Change (IPCC), 1996: *Climate Change 1995: The Science of Climate Change*. Ed. J. T. Houghton et al. Cambridge University Press, New York, 572pp.

Knyazikhin, Y. and A. Marshak, 2000: Mathematical aspects of BRDF modeling: Adjoint problem and Green's function. *Remote Sens. Rev.*, **18**, 263-280.

Leontyeva, E., and K. Stamnes, 1994: Estimations of cloud optical thickness from ground-based measurements of incoming solar radiation in the arctic. *J. Climate*, **7**, 566-578.

Li, J., 1999: Gaussian quadrature and its application to infrared radiation. *J. Atmos. Sci.*, **56**, 753-765.

Li., J., 2002: Accounting for unresolved clouds in a 1D infrared radiative transfer model. Part I: Solution for radiative transfer, including cloud scattering and overlap. *J. Atmos. Sci*, **59**, 3302-3320.

Li, J. and H. W. Barker, 2002: Accounting for unresolved clouds in a 1D infrared radiative transfer model. Part II: Horizontal variability of cloud water path. *J. Atmos. Sci.*, **59**, 3321-3339.

Marshak, A., A. B. Davis, W. J. Wiscombe, and R. F. Cahalan, 1995: Radiative smoothing in fractal clouds. *J. Geophys. Res.*, **100**, 26,247-26,261.

Marshak, A., Y. Knyazikhan, A. B. Davis, W. J. Wiscombe, and P. Pilewskie, 2000: Cloud - vegetation interaction: Use of Normalized Difference Cloud Index for estimation of cloud optical thickness. *Geophys. Res. Lett.*, **27**, 1695-1698.

Morcrette, J. -J., and Y. Fouquart, 1986: The overlapping of cloud layers in shortwave radiation parameterizations, *J. Atmos. Sci.*, **43**, 321-328.

Oreopoulos, L., and H. W. Barker, 1999: Accounting for subgrid-scale cloud variability in a multi-layer, 1D solar radiative transfer algorithm. *Q. J. R. Meteorol. Soc.*, **125**, 301-330.

Ramanathan, V., 1987: The role of Earth radiation budget studies in climate and general circulation research. *J. Geophys. Res.*, **92**, 4075-4095.

Rossow, W. B. and R. A. Schiffer, 1999: Advances in understanding clouds from ISCCP. Bull. Amer. Meteor. Soc., **80**, 2261-2287.

Rossow, W. B., C. Delo, and B. Cairns, 2002: Implications of the observed mesoscale variations of clouds for Earth's radiation budget. *J. Climate*, **15**, 557-585.

Schlesinger, M. E. and J. F. B. Mitchell, 1987: Climate model simulations of the equilibrium climatic response to increased carbon dioxide. *Review of Geophys.*, **4**, 760-798.

Stephens, G. L., 1988: Radiative transfer through arbitrary shaped optical media: Part II: Group theory and simple closures. *J. Atmos. Sci.*, **45**, 1837-1848.

Stephens, G. L., P. M. Gabriel, and S.-C. Tsay, 1991: Statistical radiative transfer in one-dimensional media and its application to the terrestrial atmosphere. Trans. Theory Stat. Phys., **20**, 139-175.

Stephens, G. L. and others, 2002: The CloudSat mission and EOS constellation: A new dimension to surface-based observations of cloud and precipitation. In press, *Bull. Am. Meteor. Soc.*

Stokes, G. M., and S. E. Schwartz, 1994: The atmospheric radiation measurement (ARM) program: Programmatic background and design of the cloud and radiation test bed. *Bull. Amer. Meteor. Soc.*, **75**, 1201-1221.

Várnai, T., and A. Marshak, 2001: Statistical analysis of the uncertainties in cloud optical depth retrievals caused by three-dimensional radiative effects. *J. Atmos. Sci.*, **58**, 1540-1548.

Welch, R. M and B. A. Wielicki, 1985: A radiative parameterization of stratocumulus cloud fields. *J. Atmos. Sci.*, **42**, 2888-2897.

Xu, K.-M. and D. A. Randall, 1996: A semiempirical cloudiness parameterization for use in climate models. *J. Atmos. Sci.*, **53**, 3084-3102.

Yu, W, L. Garand, A.P. Dastoor, 1997: Evaluation of model clouds at 100 km scale using GOES data. *Tellus*, **49A**, 246-262.